

Multi-objective optimization of water injection in spark-ignition engines using the stochastic reactor model with tabulated chemistry

International J of Engine Research

2019, Vol. 20(10) 1089–1100

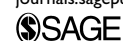
© IMechE 2019

Article reuse guidelines:

sagepub.com/journals-permissions

DOI: 10.1177/1468087419857602

journals.sagepub.com/home/ijer



Tim Franken¹ , Corinna Netzer¹ , Fabian Mauss¹,
Michal Pasternak², Lars Seidel², Anders Borg³,
Harry Lehtiniemi³, Andrea Matrisciano⁴ and
Andre Casal Kulzer⁵

Abstract

Water injection is investigated for turbocharged spark-ignition engines to reduce knock probability and enable higher engine efficiency. The novel approach of this work is the development of a simulation-based optimization process combining the advantages of detailed chemistry, the stochastic reactor model and genetic optimization to assess water injection. The fast running quasi-dimensional stochastic reactor model with tabulated chemistry accounts for water effects on laminar flame speed and combustion chemistry. The stochastic reactor model is coupled with the Non-dominated Sorting Genetic Algorithm to find an optimum set of operating conditions for high engine efficiency. Subsequently, the feasibility of the simulation-based optimization process is tested for a three-dimensional computational fluid dynamic numerical test case. The newly proposed optimization method predicts a trade-off between fuel efficiency and low knock probability, which highlights the present target conflict for spark-ignition engine development. Overall, the optimization shows that water injection is beneficial to decrease fuel consumption and knock probability at the same time. The application of the fast running quasi-dimensional stochastic reactor model allows to run large optimization problems with low computational costs. The incorporation with the Non-dominated Sorting Genetic Algorithm shows a well-performing multi-objective optimization and an optimized set of engine operating parameters with water injection and high compression ratio is found.

Keywords

Water injection, genetic optimization, spark-ignition engine, stochastic reactor model, detailed chemistry

Date received: 5 November 2018; accepted: 22 May 2019

Introduction

Water injection in combustion engines is already introduced in 1913 by Hopkinson¹ and today we experience the revival of water injection as a key technology for highly efficient spark-ignition (SI) engines.^{2–4} Water injection enables higher boost pressures and compression ratios (CRs), which result in increased engine efficiency.^{5–7} However, water injection increases the complexity of the engine since an additional injection system is needed.² To avoid frequently water refilling, water recovery systems are investigated⁸ that provide water of high purity during the engine operation but further increase the engine complexity. The rising number of engine control parameters pushes the traditional

test bench approach to its limits and demands sophisticated simulation tools to support the engine development and pre-calibration.

¹Chair of Thermodynamics and Thermal Process Engineering, Brandenburg University of Technology, Cottbus, Germany

²LOGE Deutschland GmbH, Cottbus, Germany

³LOGE AB, Lund, Sweden

⁴Chalmers University of Technology, Gothenburg, Sweden

⁵Porsche AG, Stuttgart, Germany

Corresponding author:

Tim Franken, Chair of Thermodynamics and Thermal Process Engineering, Brandenburg University of Technology, Siemens-Halske-Ring 8, 03046 Cottbus, Germany.
Email: tim.franken@b-tu.de

Detailed three-dimensional (3D) computational fluid dynamic (CFD) simulations are a common tool in engine prototype and combustion system development. Hence, researchers and engineers used 3D CFD to perform detailed studies of water injection in gasoline engines in the last years. The group of Berni et al.⁹ focused on the application of 3D CFD to investigate a port water injection concept. They showed the feasibility of the simulation approach to evaluate water effects on thermodynamic conditions and auto-ignition. With water injection they stated a reduction of brake-specific fuel consumption of 20% for a gasoline direct injection engine. Netzer et al.¹⁰ emphasize the necessity to use detailed chemistry in 3D CFD simulations, to separate physical from chemical water effects. The authors found that water effects on laminar flame speed and combustion chemistry are not negligible. Furthermore, the 3D CFD results state the strong influence of water injection and vaporization on the local distribution of temperature and auto-ignition hot spots within the cylinder. Boldaji et al.¹¹ applied direct water injection to a thermally stratified compression ignition engine using 3D CFD with detailed chemistry. They reported a decreased maximum cylinder pressure and longer combustion duration with increasing amount of injected water. Furthermore, they stated that NO_x emissions are reduced with water injection because of reduced in-cylinder temperatures. They concluded that water injection is feasible for cycle-to-cycle control for these types of engines.

While 3D CFD simulations are suitable for detailed investigations of local combustion and emission formation processes, the user has to accept high computational costs. Fast running zero-dimensional (0D)/one-dimensional (1D) simulation tools can be used to perform large SI engine parameter variations involving water injection, with low computational costs. Bozza et al.⁵ applied a 1D simulation tool to investigate the effect of cooled external exhaust gas recirculation (EGR) and water injection in a boosted SI engine. The results show a reduction of brake-specific fuel consumption for various operating conditions considering given constraints for turbine inlet temperature, boost pressure and peak cylinder pressure. The same model was applied by Bozza et al.¹² to analyze the combination of different technologies to reduce fuel consumption for Worldwide Harmonized Light Vehicles Test Cycle (WLTC) conditions. The authors stated that low pressure EGR is beneficial for low-speed and low-load operating conditions, while water injection improves fuel consumption at high-speed and high-load operating conditions enabling stoichiometric air–fuel ratios.

The physics-based quasi-dimensional (QD) SI stochastic reactor model (SRM) accounts for the mixture and temperature in-homogeneities within the cylinder.^{13–16} This approach allows to predict local

effects of fuel composition on flame propagation, auto-ignition and emission formation. The QD SRM was already applied to investigate the effect of different octane number fuels on auto-ignition in the unburned gas as shown by Netzer et al.¹⁷ The detailed chemistry for multi-component fuels used in that work as well as in the presented work is based on the methodology of reaction mechanism development and reduction introduced by Seidel and colleagues.^{18,19} To reduce the computational cost of the QD SRM simulations, Matrisciano et al.^{20,21} proposed a reaction-progress-variable-based tabulation strategy. Thereby, the detailed chemistry is pre-compiled in a look-up table based on thermodynamic conditions and reaction progress variable.

The multi-objective genetic optimization is applied to optimization problems with more than one objective and yet unknown range of the operating parameters.²² Amani et al.²³ applied multi-objective optimization to improve the water injection spray in a gas-turbine combustor. They generated response surface models (RSMs) of their optimization objectives depending on various physical parameters. Subsequently, they used the Non-dominated Sorting Genetic Algorithm (NSGA-II) together with the RSMs to perform the optimization. They stated that the optimized water spray improves the temperature non-uniformity by 19%, while the NO_x emissions are reduced by 87% minimum. Atashkari et al.²⁴ performed multi-objective optimization using neural networks of variable valve-timing SI engines and the NSGA-II. They concluded that the multi-objective optimization using neural networks is a promising approach to find optimum solutions for engine valve-timing. Ma et al.²⁵ presented a multi-objective optimization strategy using a mean-value model of a gasoline direct injection engine to predict fuel consumption and soot emissions together with the Strength Pareto Evolutionary Algorithm (SPEA). Their results showed an improvement of 3.2% of the indicated specific fuel consumption (ISFC) with the optimized engine control parameters.

The novel approach of this work is the development of a simulation-based optimization process combining the advantages of the tabulated chemistry and the NSGA-II developed by Deb et al.^{26,27} implemented in the modeFRONTIER software package.²⁸ The optimization objectives are the reduction of fuel consumption and knock probability of a SI engine operating point with water injection. The first section of this article introduces the fundamentals of the QD SRM and the tabulated chemistry. Then, the numerical test case from 3D CFD simulation is presented. The simulation-based optimization process is outlined in the subsequent section, which contains a description of the calculation of the scalar mixing time using turbulent kinetic energy from 3D CFD and the modeling of the port water

injection. Finally, the optimization results are discussed, followed by the conclusions and outlook of future work.

SRM

The QD SRM is based on a probability density function (pdf) approach for reactive flows.^{29–31} The transport equation (1) of the pdf contains on the left side the accumulation term and various source terms $Q_i(\psi)$. These source terms include the piston work, convective heat transfer, chemical reactions, direct injection and vaporization. Therein, Φ is a vector of random variables, ψ is its realization in the sample ψ -space and t is the time. The term on the right side P_2 describes the molecular mixing due to turbulence and is in a non-closed form

$$\frac{\partial}{\partial t} F_{\Phi}(\psi, t) + \frac{\partial}{\partial \psi_i} (Q_i(\psi) F_{\Phi}(\psi, t)) = P_2 F_{\Phi}(\psi, t) \quad (1)$$

The Curl³² mixing model is incorporated to close the term P_2 in equation (2). The mixing model contains the turbulent mixing time τ , to account for turbulence–chemistry interaction,^{13,14} the calibration parameter C_{Φ} and the decay parameter β , which is set to 1

$$P_2 F_{\Phi}(\psi, t) = \frac{C_{\Phi} \beta}{\tau} \left[\int_{\Delta\psi} F_{\Phi}(\psi - \Delta\psi, t) F_{\Phi}(\psi + \Delta\psi) d(\Delta\psi) - F_{\Phi}(\psi, t) \right] \quad (2)$$

To solve the pdf transport equation, the gas within the cylinder is discretized in notional particles, each containing its own composition and temperature (see Figure 1).

The QD SRM uses a two-zone approach and the auto-ignition in the end gas and chemistry in the burned zone for emission formation are retrieved using tabulated chemistry. The flame front propagates based on turbulent flame speed s_T , which is calculated retrieving the laminar flame speed s_L from the pre-compiled look-up tables. The turbulent flame speed is calculated with equation (3) based on the model by Kolla et al.³³ and introduced for the QD SRM by Bjerkborn et al.³⁴

$$\frac{s_T}{s_L} = \sqrt{\frac{18C_{\mu}}{(2C_m - 1)\beta'} \left((2K_C^* - \tau C_4) \frac{l_L u'}{\delta_L s_L} + C_3 \frac{2}{3} \left(\frac{u'}{s_L} \right)^2 \right)} \quad (3)$$

Therein, β' , K_C^* , C_{μ} , C_m , C_4 and C_3 are model constants. τ is a coefficient defined as $\tau = ((T_{ad} - T_{ub})/T_{ub})$ with the adiabatic temperature T_{ad} and the temperature of the unburned zone T_{ub} . l_L is the integral length scale and δ_L is the thickness of the flame front. u' is the turbulence intensity. In addition, the flame front is traced based on a polygonal approach to account for

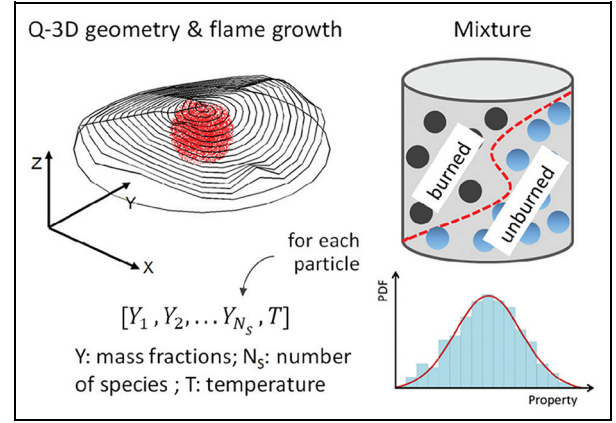


Figure 1. Concept of the two-zone stochastic reactor model for spark-ignition engines.¹³

Table 1. QD SRM model setup.

Number of particles	200
Time step size	1 °CA
Number of cycles	5
C_{Φ}	0.83
C_{pre}	1.0
Woschni C_1	2.28
Woschni C_2	0.0035

QD: quasi-dimensional; SRM: stochastic reactor model.

flame–wall interactions (see Q-3D geometry and flame growth in Figure 1). The QD SRM accounts for cycle-to-cycle variations in the cylinder gas composition and temperature induced by stochastic mixing and heat transfer processes. The Woschni heat transfer correlation in equation (4) with base parameters and wall temperatures of 450 K is used to calculate the heat transfer coefficient α

$$\alpha = C_{pre} \cdot d^{-0.2} \cdot p^{0.8} \cdot T^{-0.53} \cdot \left[C_1 \cdot c_m + C_2 \frac{V \cdot T_0}{p_0 \cdot V_0} \cdot (p - p_{mot}) \right] \quad (4)$$

Therein, C_{pre} , C_1 and C_2 are model constants; d is the engine bore; p is the cylinder pressure; T is the cylinder temperature; c_m is the mean piston speed; p_{mot} is the motored cylinder pressure; and V is the cylinder volume. The index 0 highlights parameters at reference conditions. The QD SRM final model setup used for the multi-objective optimization is shown in Table 1.

The pdf transport equation (1) is solved using an operator split method outlined in Figure 2.¹⁶ At the end of each operator split loop, a pressure correction is performed.

Tabulated chemistry

The tabulated chemistry is based on the detailed ETRF (ethanol toluene reference fuel) reaction scheme

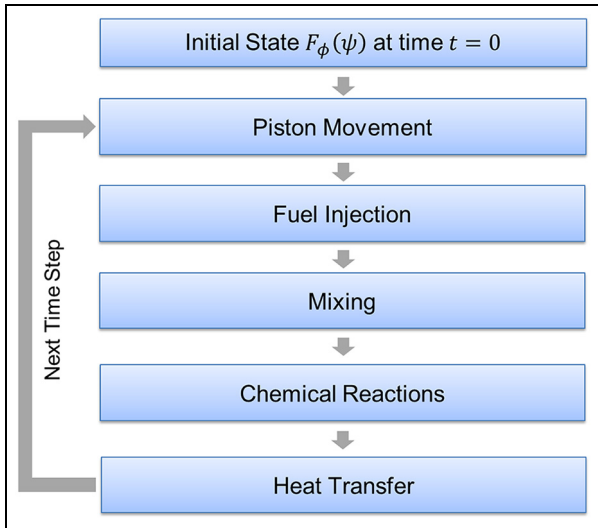


Figure 2. QD SRM numerical solution method.

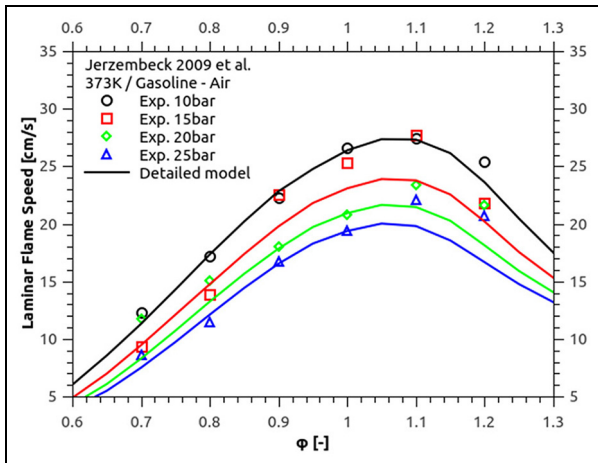


Figure 3. Comparison of predicted laminar flame speeds using the detailed reaction scheme by Seidel¹⁸ and experiments with gasoline as fuel from Jerzembeck et al.³⁵ at 373 K and different pressures, with air as oxidizer. Measurement accuracy is within ± 4 cm/s. The symbols highlight the experiments and the lines show the simulations.

developed by Seidel¹⁸ consisting of 475 species and 5160 reactions. The detailed reaction scheme is validated for different experiments and for engine relevant conditions, which is highlighted for one set of experiments from Jerzembeck et al.³⁵ in Figure 3.

The influence of water vapor on the laminar flame speed is outlined in Figure 4. Therein, the experimental results by Mazas et al.³⁶ using methane as fuel are compared with flame speed simulations using the detailed reaction scheme developed by Seidel.¹⁸ With increasing amount of water vapor, the flame speed is reduced, which is accurately predicted by the simulations. Similar trends of the laminar flame speed are reported by Liang et al.³⁷ for ethanol-water mixtures and by Vancoillie et al.³⁸ for methanol-water mixtures. The sensitivity of the detailed reaction scheme toward water

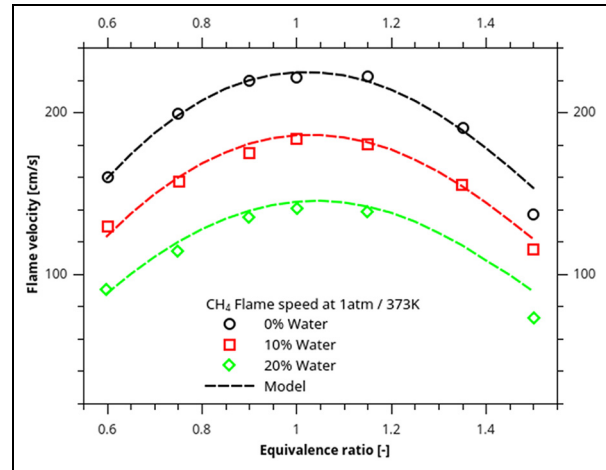


Figure 4. Comparison of predicted laminar flame speeds using the detailed reaction mechanism by Seidel¹⁸ and experiments from Mazas et al.³⁶ with methane as fuel and different steam content at 1 atm, 373 K, with air as oxidizer. The symbols highlight the experiments and the dashed lines show the simulations.

Table 2. Laminar flame speed dual fuel table specifications.

	Range	Steps
Temperature	350–1200 K	50 K
Pressure	1–100 bar	1 bar
Equivalence ratio	0.5–1.5	0.05
Water/fuel ratio	0%–60%	10%
EGR	0%–20%	10%

EGR: exhaust gas recirculation.

Table 3. Combustion chemistry dual fuel table specifications.

	Range	Steps
Temperature	250–1400 K	25 K
Pressure	1–200 bar	2.5 bar
Equivalence ratio	0.2–4.0	0.2
Water/fuel ratio	0%–50%	10%
EGR	0%–30%	10%

EGR: exhaust gas recirculation.

vapor is investigated in the publication by Netzer et al.¹⁰ Therein, the influence of water on the thermodynamics and chemistry is analyzed before, during and after the combustion process. The authors concluded that water vapor has a distinct impact on the laminar flame speed, the ignition delay time and the equilibrium of the chemical reactions. Thus, water vapor influences need to be accounted for by a suitable reaction scheme.

The laminar flame speeds and the combustion chemistry are stored in pre-compiled look-up tables (see table ranges in Tables 2 and 3). A dual fuel approach for the ETRF surrogate and water is used. The first fuel stream is composed of 5.3% ethanol, 49.2% iso-octane, 9.1%

Table 4. Engine geometry and operating conditions for the base case without water presence.

Bore × stroke	86 mm × 90 mm
Rod	180 mm
Compression ratio	10:1
Intake valve closure	−100.5 °CA aTDC
Exhaust valve opening	120 °CA aTDC
Spark timing	−4 °CA aTDC
Fuel mass	57 mg/cycle
Equivalence ratio	1.02

aTDC: after top dead center.

n-heptane and 36.4% toluene in mass percent. The second fuel stream is composed of 100% water. During the simulation, laminar flame speeds and chemistry sources are retrieved from the look-up tables based on the current thermodynamic conditions.

Furthermore, a progress variable approach is used for the chemistry table look-up.^{20,21,39,40} The progress variable C is defined as follows

$$C = \frac{h_{298} - h_{298,0}}{h_{298,eq} - h_{298,0}} \quad (5)$$

where h_{298} is the current chemical enthalpy, $h_{298,0}$ is the enthalpy of formation at standard state and $h_{298,eq}$ is the chemical enthalpy in equilibrium.⁴¹ The fuel–water–air mixture is initialized homogeneously mixed at the start of the QD SRM simulation, assuming an idealized port-injection.

Numerical test case

The 3D CFD test case for a boosted SI engine operating point at 2500 r/min and 16.2 bar indicated mean effective pressure (IMEP) from Netzer et al.¹⁰ is used to perform the multi-objective optimization with the QD SRM and tabulated chemistry. The engine geometry and operating conditions are listed in Table 4. The base case without water presence is used for calibration of the QD SRM mixing time. In addition, three operating points with different spark timings, water/fuel (w/f) ratios (20%, 50% and 80% w/f ratio) and IMEPs are used to validate the QD SRM.

Simulation-based optimization process

The novel approach of this work is the development of a simulation-based optimization process combining the advantages of the tabulated chemistry, the QD SRM and the NSGA-II. The optimization process is outlined in Figure 5.

The detailed ETRF reaction scheme was used for the 3D CFD simulations and is further used to generate the tabulated chemistry for the QD SRM simulations. The turbulent kinetic energy k_{CFD} shown in Figure 6 is extracted from the 3D CFD simulation and used in conjunction with the integral length scale

function⁴² to calculate the QD SRM mixing time τ in equation (6)

$$\tau = \frac{\left(\frac{6V}{\pi}\right)^{\frac{1}{3}}}{\sqrt{\frac{2}{3}} \cdot k_{CFD}} \quad (6)$$

where V is the instantaneous cylinder volume and C_ϕ is the calibration parameter for the QD SRM mixing time. To account for the changes of thermodynamic conditions due to water injection and vaporization, a simplified approach is used.^{43,44} The water mass and vaporization enthalpy of water at 100 °C ($q_{vap,water} = 2264$ kJ/kg)⁴⁵ are used to calculate the energy Q_{water} needed to vaporize the liquid water. Then, based on the isobaric heat capacity of air ($c_{p,air} = 1.008$ kJ/kg K)⁴⁵ and trapped mass $m_{trapped}$, the temperature drop ΔT of the cylinder gas temperature is calculated in equation (7)

$$\Delta T = \frac{Q_{water}}{c_{p,air} \cdot m_{trapped}} \quad (7)$$

To evaluate the knock probability, the knock limit is defined as 6 J/°CA maximum heat release rate in the unburned zone in the QD SRM (see Figure 7). The engine case used is found to be at the knock limit in the previous study published by Netzer et al.¹⁰ The authors used the Detonation Diagram to evaluate the auto-ignition.^{17,46–48} Therefore, the heat release rate in the unburned zone of this case is used as threshold. The base case without knock is highlighted with the bold red line, which shows the characteristic heat release rate profile with the low temperature heat release at 15 °CA aTDC and the auto-ignition heat release rate at 37 °CA aTDC. In comparison, the significantly higher unburned zone heat release rate of a knocking case is shown with the thin red line.

For the multi-objective optimization the NSGA-II coupled with RSMs and the uniform Latin hypercube (ULHC) space filler algorithm is applied²⁸ (see Figure 8). The RSMs including neural networks, Kriging models and polynomial functions are trained based on the already existing design database and the best performing RSM is selected. The RSM is used to perform additional internal exploration and optimization tasks during the multi-objective optimization. With that approach, the number of optimization steps is increased, without additional QD SRM runs, leading to a well-defined Pareto Front and less computational costs. The Pareto Front is a result of the multi-objective optimization, which contains the optimum solutions of the objectives, where no better solutions exist.²⁸ The RSM-coupled optimization process is repeated for each new generation.

The number of designs is set to 10 and the number of generations is set to 150. In total, 1500 designs are evaluated during the multi-objective optimization. The optimization objectives are the reduction of the fuel mass and the maximum heat release rate in the unburned

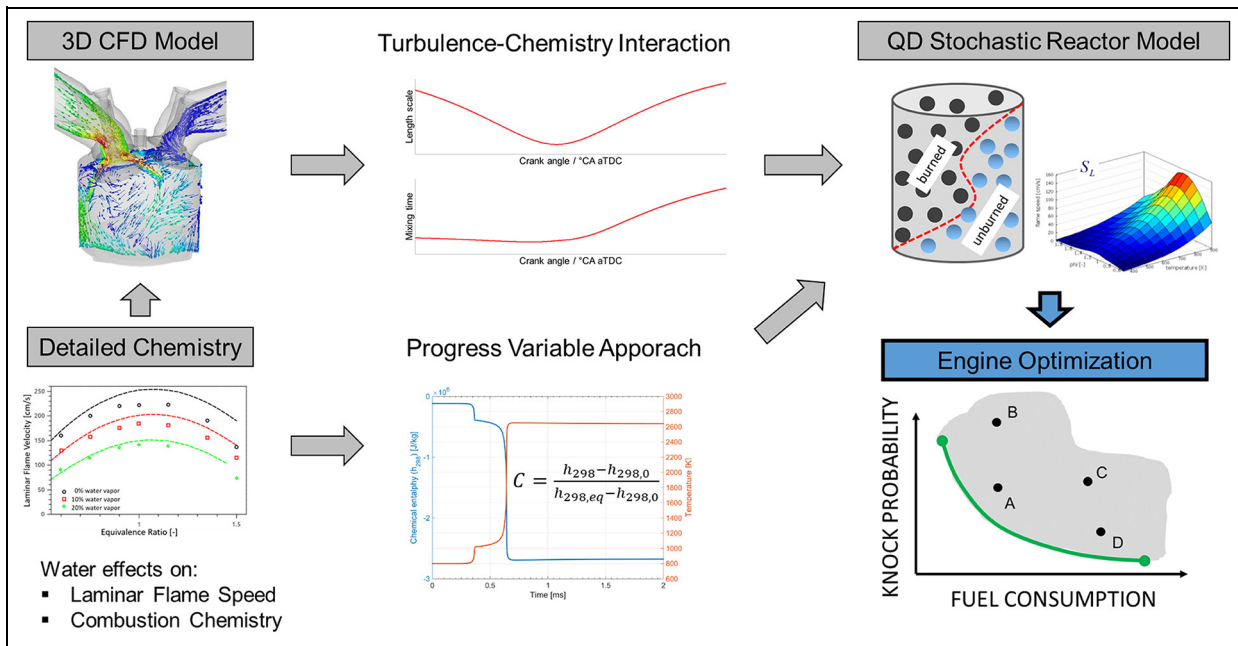


Figure 5. QD SRM and 3D CFD simulation-based optimization process with tabulated chemistry.

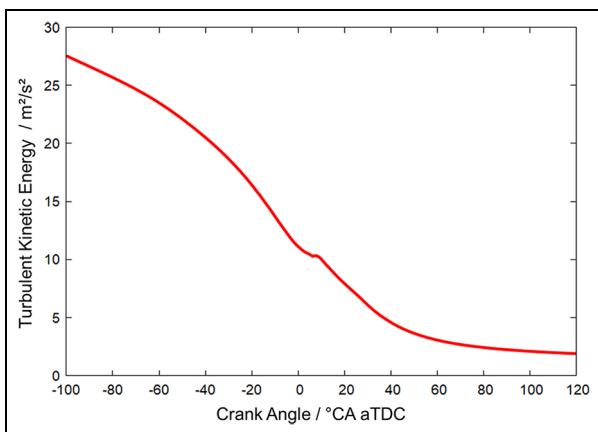


Figure 6. Mass-averaged turbulent kinetic energy of 3D CFD.

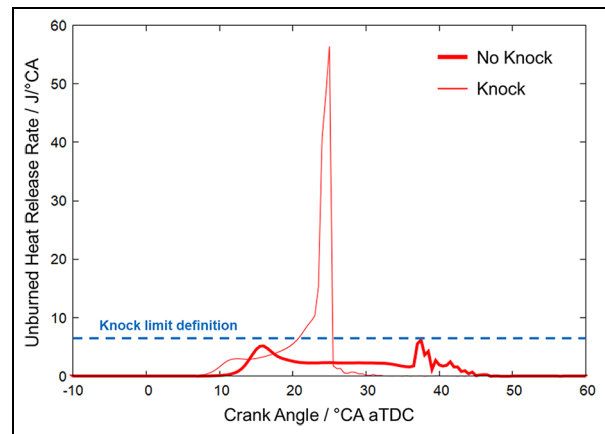


Figure 7. Knock limit definition in QD SRM for multi-objective optimization.

zone. The optimization input parameters and their ranges are shown in Table 5. To compare the cases at the same engine load, the IMEP is constrained to deviate within a range of $\pm 3\%$.

Results and discussion

The QD SRM calibration and validation results for cylinder pressure, heat release rate and exhaust emissions (CO_2 , H_2O , CO and NO_x) compared to 3D CFD are shown in Figure 9. The calibration case (a) shows a good agreement with the 3D CFD results. For the first validation case (b) with 20% w/f ratio, the spark timing was shifted to earlier crank angles in 3D CFD; therefore, the maximum cylinder pressure is as high as for the base case. For the validation cases (c) with 50% w/f ratio and (d) with 80% w/f ratio, the maximum

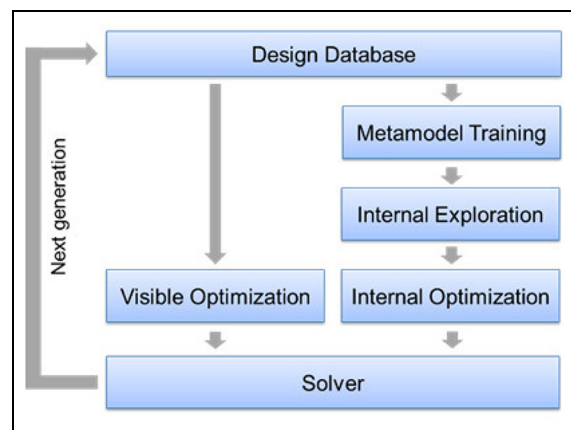


Figure 8. Multi-objective optimization with the NSGA-II and RSMs.

Table 5. Multi-objective optimization design parameter ranges.

	Minimum	Maximum
Compression ratio	9:1	13:1
Water/fuel ratio	0%	40%
Pressure at IVC	1.7 bar	2.7 bar
Spark timing	-25 °CA aTDC	5 °CA aTDC

IVC: intake valve closure; aTDC: after top dead center.

cylinder pressure is decreasing due to a longer combustion duration in QD SRM and 3D CFD. All cases show a good agreement for the predicted exhaust emissions at exhaust valve opening (EVO). Overall, the QD SRM matches the 3D CFD results accurately and the applicability of the proposed mixing time modeling approach is proven. Subsequently, the validated QD

SRM is used for the multi-objective optimization of the 3D CFD SI engine operating point.

The overall optimization time for the one operating point and the 1500 designs is 6 h and 45 min on three cores of an Intel i7-7820HQ CPU at 2.90 GHz. The multi-objective optimization is able to find an optimum solution and the resulting Pareto Front is shown in Figure 10. On the *x*-axis, the fuel mass and on the *y*-axis the maximum heat release rate (uHRR) in the unburned zone are plotted. The designs of the Pareto Front are highlighted with the black circle symbol showing the trade-off between fuel mass and uHRR. The designs are grouped into two clusters (low knock probability and low fuel consumption), highlighted by the dark and light gray colored ellipses. The designs within these clusters share similar optimized engine operating parameters. The engine operating parameters are highlighted in Figure 11, which shows the two

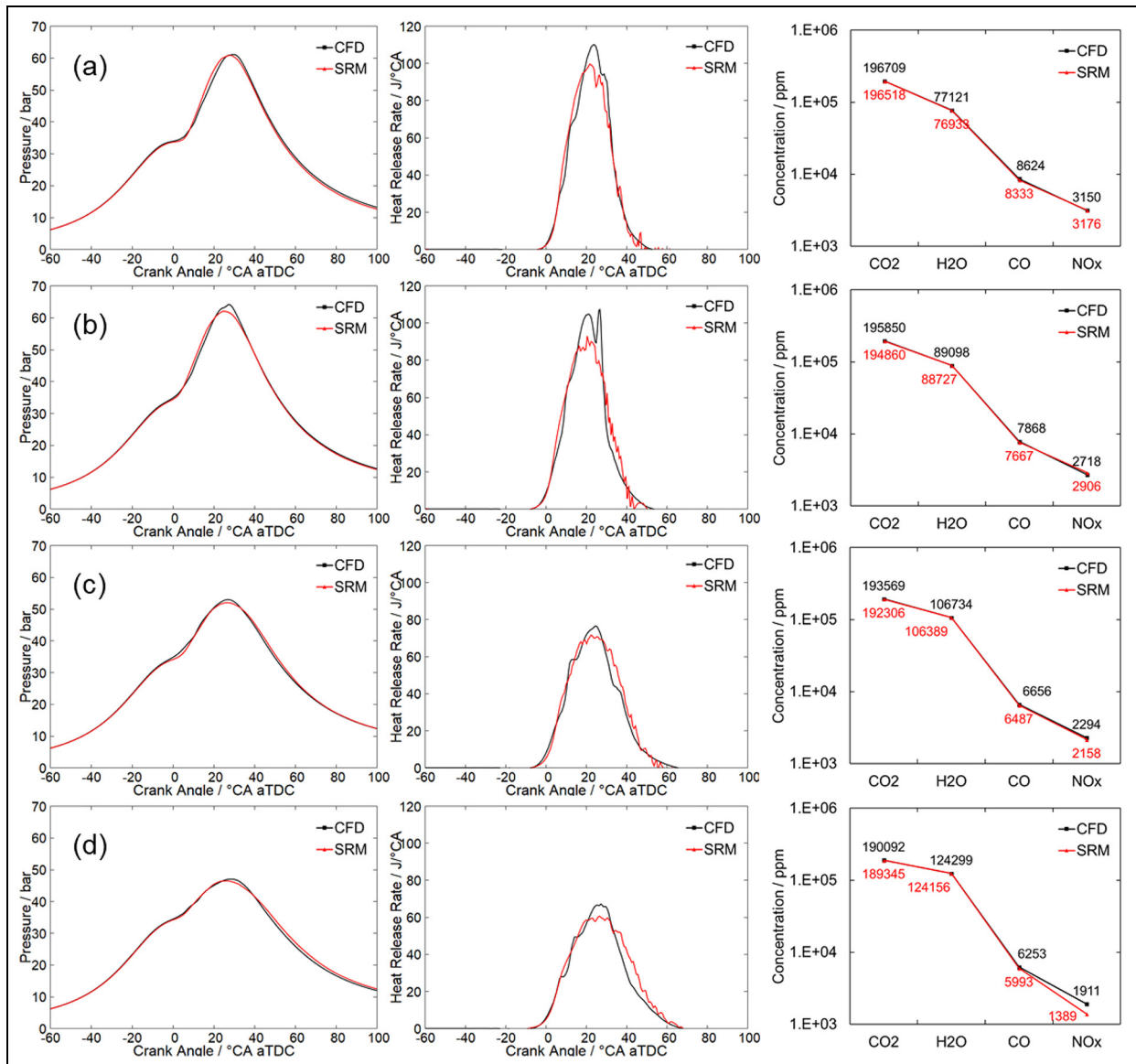


Figure 9. 3D CFD and QD SRM with detailed chemistry. Calibration results for case (a) with 0% w/f ratio and 16.2 bar IMEP and the validation results for the cases (b) with 20% w/f ratio and 16.2 bar IMEP, (c) with 50% w/f ratio and 15 bar IMEP and (d) with 80% w/f ratio and 14.1 bar IMEP.

clusters in dark and light gray and the base case in red color. In addition, the variation ranges of each operating parameter are shown for the two clusters.

The low fuel consumption cluster consists of designs with high CRs, high w/f ratios, low pressure at intake valve closure (IVC), advanced spark timing and low temperature at IVC compared to the base case. In the literature, it is well stated⁴⁹ that due to the increase in the CR, the thermal efficiency of the engine is improved and the ISFC is decreased. The pressure at IVC is decreased since it controls how much mass, containing the air mass and port injected fuel mass, is trapped in the cylinder. The equivalence ratio is kept constant for all optimization designs, using the value from Table 4. The high w/f ratio limits the further increase of uHRR, which in average is already higher compared to the base case. The high amount of water leads to a cool down of the intake air and lower temperatures at IVC. In addition, the spark timing is further advanced and the crank angle of 50% mass fraction burned is found at 8 °CA aTDC in the region of highest thermal efficiency.

The low knock probability cluster includes designs with moderate CR, high w/f ratio, close-to-base pressure at IVC, retarded spark timing and low temperature at IVC. The moderate CR and the retarded spark timing are beneficial for low knock probability because they favor low gas temperatures in the unburned zone. Furthermore, the high w/f ratios cool down the unburned gas temperature and slow down the chemical reactions in the unburned zone, which decreases the knock probability. As a consequence, the thermal efficiency is decreased and the fuel consumption is slightly increased compared to the base case.

In the next step, four cases are selected from the Pareto Front, which are highlighted in Figure 10 and these points are analyzed more in detail. The cylinder pressure, the heat release rate in the unburned zone and the deviation of exhaust emission masses compared to the base case are shown in Figure 12. The optimized engine parameters of the five cases including the CR, the w/f ratio, the spark timing (θ_{ST}) and the temperature at IVC (T_{IVC}) are summarized in Table 6.

The best case is depicted in Figure 12(a) showing a higher compression pressure due to a higher CR (see Table 6), an advanced spark timing and increased peak cylinder pressure of 130 bar. The optimized parameters increase the thermal efficiency of the engine and as a result decrease the fuel consumption. Due to the improved combustion, the heat release rate in the unburned zone is increased, which leads to a higher knock probability. The heat release rate in the unburned zone exceeds the knock limit, defined in Figure 7, and is therefore not feasible. The increased w/f ratio in this case limits the increase of the heat release rate in the unburned zone to a higher level. Similar trends are also reported by Worm et al.⁵⁰ and Teodosio et al.⁵¹ With the best case the CO₂ and NO_x emissions are predicted to decrease, while the CO emissions are

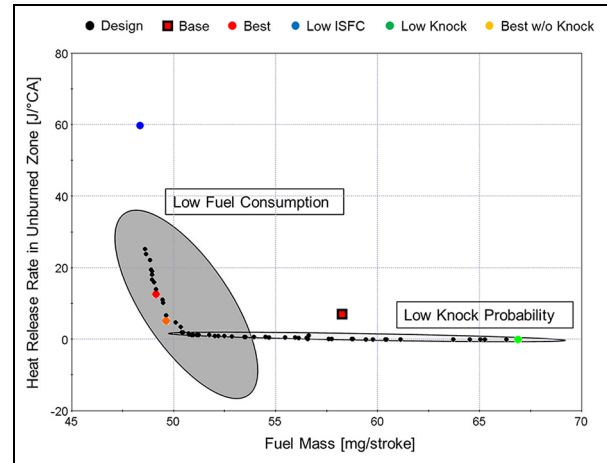


Figure 10. QD SRM optimization results with tabulated chemistry. The dark and light gray colored ellipses highlight clusters of designs sharing similar sets of engine parameters.

increased. Compared to the results reported by Marchitto et al.⁵² and Teodosio et al.,⁵³ the emission trends are opposite. The group by Iacobacci et al.⁵⁴ measured the same emission trends as presented in this work. It has to be noted that the engine settings in these cases differ, which can lead to the differences in the emission trends. The low knock case in Figure 12(b) shows a delayed combustion because of retarded spark timing and moderate CR. Together with the increased w/f ratio, the heat release rate in the unburned zone is almost zero and the knock probability is low. The CO₂ and CO emissions are increased, while the NO_x emissions are decreased due to the delayed combustion and the reduced maximum cylinder temperatures. The low ISFC case in Figure 12(c) indicates similar settings as the best case with the difference that the w/f ratio is lower. This reduction and the increase in temperature at IVC promote a strong increased heat release rate in the unburned zone with a high potential of knocking combustion. Furthermore, the NO_x and CO emissions are increased for the low ISFC case, while the CO₂ emissions are decreased because of less fuel consumption. The base case without knocking combustion in Figure 12(d) has a retarded spark timing compared to the best case; therefore, the heat release rate in the unburned zone is reduced and the knock probability is low. The emission trends are similar compared to the best case, with decreased CO₂ and NO_x emissions and increased CO emissions.

To highlight the advantage of the QD SRM simulation with tabulated chemistry, the computational times of three different cases are compared. The computational time of the 3D CFD simulation for one closed-engine-cycle is 16 h on 24 cores. The QD SRM with online chemistry (chemical reactions are solved during the simulation run) takes 3 min for one closed-engine-cycle on 16 cores. Finally, the QD SRM with tabulated chemistry takes 3 s for one closed-engine-cycle on one

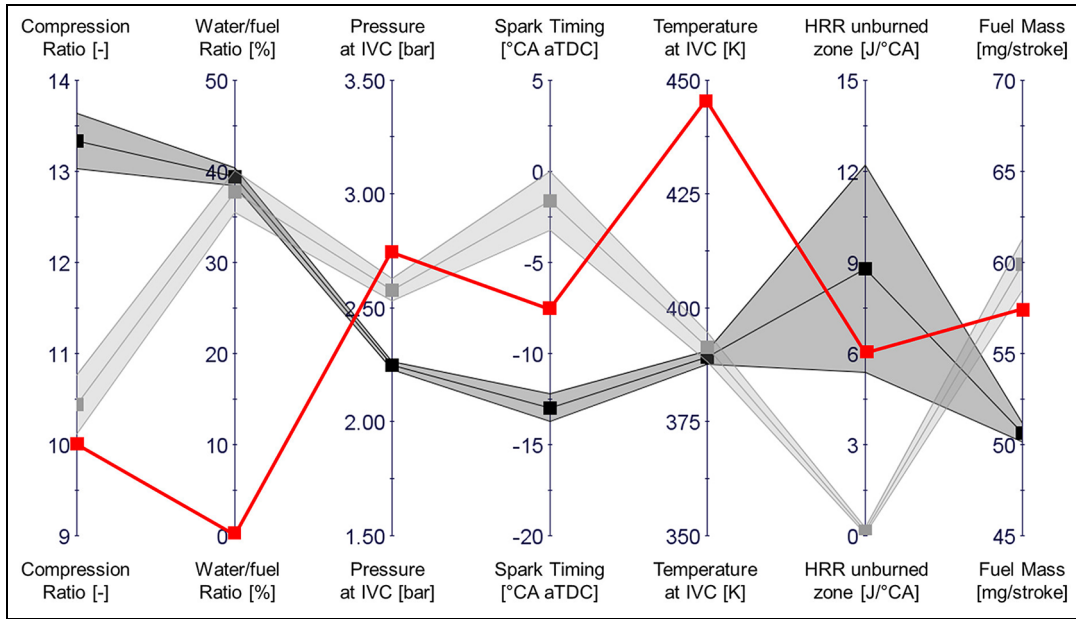


Figure 11. QD SRM optimization results with tabulated chemistry. The red line shows the base engine parameter values. The black and gray colored lines highlight the average engine parameter values for Cluster-1 and Cluster-2.

Table 6. Optimized engine operating parameters.

	CR	WF	θ_{ST}	T_{IVC}
Base	10.0	0%	-4.0 °CA	445 K
Best	14.0	42.5%	-16.88 °CA	385 K
Low ISFC	14.0	28.2%	-15.38 °CA	405 K
Low knock	9.6	43%	4.61 °CA	384 K
Best case without knock	14.0	43%	-14.4 °CA	384 K

CR: compression ratio; WF: water/fuel ratio; ISFC: indicated specific fuel consumption; IVC: intake valve closure.

core, while the prediction accuracy is similar to the online chemistry case.²⁰

Conclusion

A novel simulation-based optimization process using a genetic algorithm with different constraints and targets was successfully applied for the assessment of water injection in turbocharged SI engines. The process includes tabulated chemistry, the QD SRM and the NSGA-II for multi-objective optimization of fuel consumption and knock probability. The 3D CFD simulation results of a 2500 r/min and 16.2 bar IMEP operating point are used as reference. The following conclusions are drawn from the optimization results:

- The QD SRM with tabulated chemistry is a fast running simulation tool, which can be used for large optimization problems. It incorporates physics-based sub-models, detailed chemistry and accounts for mixture and temperature inhomogeneity, which improves its predictive capability for combustion and emissions compared to common mean-value models.

- The NSGA-II coupled with RSMs and using the ULHC space filler algorithm is a robust and well-performing multi-objective optimization tool. It allows to reduce the number of optimization steps with the QD SRM, while the prediction of the Pareto Front is still accurate.
- The general knowledge from SI engine development could be confirmed by the QD SRM multi-objective optimization. The reduction of fuel consumption is favored by increased CR and earlier spark timing. In contrast, the lower knock probability is influenced by low CRs and later spark timings.
- The presence of water is beneficial for reducing fuel consumption and knock probability at the same time. An optimum w/f ratio in the range of 40% is determined from the QD SRM optimization.

The future work includes the following items:

- Currently running single-cylinder SI engine experiments will be used to further validate the integrated simulation-based optimization process.
- The QD SRM with tabulated chemistry will be applied to other engine cases and its predictive

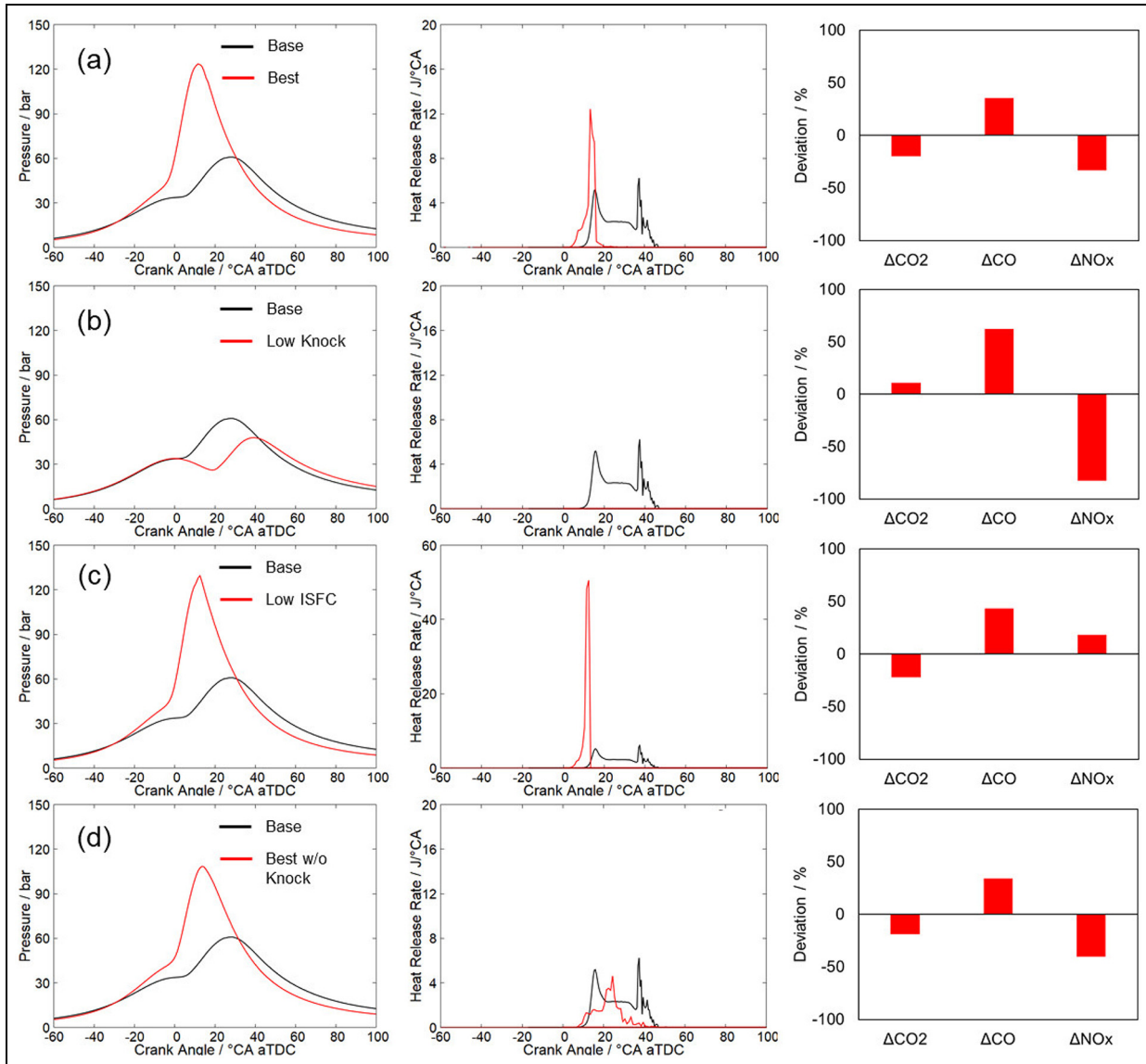


Figure 12. QD SRM optimization results with tabulated chemistry. The cylinder pressure, unburned zone heat release rate and deviation of emissions for (a) the best case, (b) the lowest knock case, (c) the lowest fuel consumption and (d) the best case without knock.

capability of exhaust emissions will be evaluated.

- The water injection and vaporization model in QD SRM will be extended for direct water injection. The thermodynamic equations in the model will be improved to account for the different calorific properties of the liquid and vaporized water for different thermodynamic conditions and include the water vapor saturation described by Vaudry.⁴⁴
- A phenomenological K-k- ϵ turbulence model^{55–57} will be implemented in QD SRM to predict the scalar mixing time for different engine operating conditions without using information from 3D CFD simulations.

Acknowledgements

The presented work is carried out within the FVV research project “Water Injection in SI Engines.” The FVV research project is performed by the Brandenburg University of Technology at the Chair of Thermodynamics, by the Technical University Berlin at the Department of Internal Combustion Engines and by the University of Stuttgart at the Institute for Internal Combustion Engines and Automotive.


Declaration of conflicting interests


The author(s) declared no potential conflicts of interest with respect to the research, authorship and/or publication of this article.

Funding

The author(s) disclosed receipt of the following financial support for the research, authorship and/or publication of this article: The project was funded by the FVV from own resources and conducted by an expert group under the direction of Dr-Ing. Andre Kulzer, Porsche AG. The authors gratefully acknowledge the support received from the Research Association for Combustion Engines (FVV) eV and from all project participants.

ORCID iDs

Tim Franken  <https://orcid.org/0000-0003-1282-1714>

Corinna Netzer  <https://orcid.org/0000-0002-4445-7243>

References

- Hopkinson B. A new method of cooling gas-engines. *Proc IMechE* 1913; 85(1): 679–715.
- Durst B, Unterweger G, Rubbert S, Witt A and Böhm M. Thermodynamic effects of water injection on otto cycle engines with different water injection systems. In: *The working process of the internal combustion engine*, Graz, 24–25 September 2015. Graz: University of Technology Graz.
- Heinrich C, Dörksen H, Esch A and Krämer K. Gasoline water direct injection (GWDI) as a key feature for future gasoline engines. In: Günther M and Sens M. (eds) *Knocking in gasoline engines*. Cham: Springer, 2018, pp.322–337.
- De Bellis V, Bozza F, Teodosio L and Valentino G. Experimental and numerical study of the water injection to improve the fuel economy of a small size turbocharged SI engine. SAE technical paper 2017-01-0540, 2017.
- Bozza F, De Bellis V and Teodosio L. Potentials of cooled EGR and water injection for knock resistance and fuel consumption improvements of gasoline engines. *Appl Energ* 2016; 169: 112–125.
- Hoppe F, Thewes M, Baumgarten H and Dohmen J. Water injection for gasoline engines: potentials, challenges, and solutions. *Int J Eng Res* 2016; 17(1): 86–96.
- Valero-Marco J, Lehrheuer B, Lopez JJ and Pischinger S. Potential of water direct injection in a CAI/HCCI gasoline engine to extend the operating range towards higher loads. *Fuel* 2018; 231: 317–327.
- Sung Y, Fischer M, Bradford M and Kotrba A. Water recovery from gasoline engine exhaust for water injection. SAE technical paper 2018-01-0369, 2018.
- Berni F, Breda S, Lugli M and Cantore G. A numerical investigation on the potentials of water injection to increase knock resistance and reduce fuel consumption in highly downsized GDI engines. *Energ Proc* 2015; 81: 826–835.
- Netzer C, Franken T, Seidel L, Lehtiniemi H and Mauss F. Numerical analysis of the impact of water injection on combustion and thermodynamics in a gasoline engine using detailed chemistry. *SAE Int J Eng* 2018; 11: 1151–1166.
- Boldaji MR, Sofanopoulos A, Mamalis S and Lawler B. Effects of mass, pressure, and timing of injection on the efficiency and emissions characteristics of TSCI combustion with direct water injection. SAE technical paper 2018-01-0178, 2018.
- Bozza F, De Bellis V, Teodosio L, Tufano D and Malfi E. Techniques for CO₂ emission reduction over a WLTC. A numerical comparison of increased compression ratio, cooled EGR and water injection. SAE technical paper 2018-37-0008, 2018.
- Pasternak M, Mauss F, Sens M, Riess M, Benz A and Stapf KG. Gasoline engine simulations using zero-dimensional spark ignition stochastic reactor model and three-dimensional computational fluid dynamics engine model. *Int J Eng Res* 2016; 17(1): 76–85.
- Sens M, Benz A, Riess M, Lage FG, Bjerkborn XS, Mauss F, et al. Multiple spark plug approach: potential for future highly diluted spark ignited combustion. In: *SIA powertrain*, Versailles, 27–28 May 2015. Suresnes: Société des Ingénieurs de l'Automobile.
- Pasternak M, Netzer C, Mauss F, Fischer M, Sens M and Riess M. Simulation of the effects of spark timing and external EGR on gasoline combustion under knock-limited operation at high speed and load. In: *International conference on knocking in gasoline engines*, Berlin, 12–13 December 2017. Cham: Springer.
- Loge AB. *Scientific software for modelling of chemical kinetic systems*, http://logesoft.com/loge-16/wp-content/uploads/2017/10/Manual_LicenseSetup.pdf
- Netzer C, Seidel L, Pasternak M, Klauer C, Perlman C, Ravet F, et al. Engine knock prediction and evaluation based on detonation theory using a quasi-dimensional stochastic reactor model. SAE technical paper 2017-01-0538, 2017.
- Seidel L. *Development and reduction of a multicomponent reference fuel for gasoline*. PhD Thesis, 2017. Cottbus: Brandenburg University of Technology Cottbus-Senftenberg.
- Seidel L, Netzer C, Hilbig M, Mauss F, Klauer C, Pasternak M, et al. Systematic reduction of detailed chemical reaction mechanisms for engine applications. *J Eng Gas Turb Power* 2017; 139(9): 091701.
- Matrisciano A, Franken T, Perlman C, Borg A, Lehtiniemi H and Mauss F. Development of a computationally efficient progress variable approach for a direct injection stochastic reactor model. SAE technical paper 2017-01-0512, 2017.
- Matrisciano A, Borg A, Perlman C, Lehtiniemi H, Pasternak M and Mauss F. Soot source term tabulation strategy for diesel engine simulations with SRM. SAE technical paper 2015-24-2400, 2015.
- Konak A, Coit DW and Smith AE. Multi-objective optimization using genetic algorithms: a tutorial. *Reliab Eng Syst Safe* 2006; 91: 992–1007.
- Amani E, Akbari MR and Shahpouri S. Multi-objective CFD optimizations of water spray injection in gas-turbine combustors. *Fuel* 2018; 227: 267–278.
- Atashkari K, Nariman-Zadeh N, Gölcü M, Khalkhali A and Jamali A. Modelling and multi-objective optimization of a variable valve-timing spark-ignition engine using

- polynomial neural networks and evolutionary algorithms. *Energ Conv Manage* 2007; 48: 1029–1041.
25. Ma H, Li Z, Tayarani M, Lu G, Xu H and Yao X. Model-based computational intelligence multi-objective optimization for gasoline direct injection engine calibration. *Proc IMechE, Part D: J Automobile Engineering* 2018; 233: 1391–1402.
 26. Deb K, Pratap A, Agarwal S and Meyarivan T. A fast and elitist multiobjective genetic algorithm: NSGA-II. *IEEE T Evolut Comput* 2002; 6(2): 182–197.
 27. Deb K, Pratap A, Agarwal S and Meyarivan T. A fast elitist non-dominated sorting genetic algorithm for multi-objective optimization: NSGA-II. In: Schoenauer M, Deb K, Rudolph G, Yao X, Lutton E, Merelo JJ and Schwefel H-P. (eds) *Parallel problem solving from nature PPSN VI*. Berlin: Springer, 2000, pp.849–858.
 28. ESTECO SpA. *modeFRONTIER User Guide*, 2017R4. Trieste: ESTECO SpA, 2017.
 29. Kraft M. *Stochastic modeling of turbulent reacting flow in chemical engineering*. Düsseldorf: VDI-Verlag, 1998.
 30. Tuner M, Pasternak M, Mauss F and Bensler H. A pdf-based model for full cycle simulation of direct injected engines. SAE technical paper 2008-01-1606, 2008.
 31. Pasternak M. *Simulation of the diesel engine combustion process using the stochastic reactor model*. PhD Thesis, 2016. Cottbus: Brandenburg University of Technology Cottbus-Senftenberg.
 32. Curl RL. Dispersed phase mixing: I theory and effects in simple reactors. *AIChE J* 1963; 9(2): 175–181.
 33. Kolla H, Rogerson JW, Chakraborty N and Swaminathan N. Scalar dissipation rate modeling and its validation. *Combust Sci Technol* 2009; 181(3): 518–535.
 34. Bjerkborn S, Perlman C, Fröjd K and Mauss F. A Monte Carlo based turbulent flame propagation model for predictive SI in-cylinder engine simulations employing detailed chemistry for accurate knock prediction. *SAE Int J Eng* 2012; 5: 1637–1647.
 35. Jerzembeck S, Peters N, Pepiot-Desjardins P and Pitsch H. Laminar burning velocities at high pressure for primary reference fuels and gasoline: experimental and numerical investigation. *Combust Flame* 2009; 156: 292–301.
 36. AN Mazas, B Fiorina, DA Lacoste and T Schuller. Effects of water vapor addition on the laminar burning velocity of oxygen-enriched methane flames. *Combustion and Flame* 2011; 158: 2428–2440.
 37. Liang J, Li G, Zhang Z, Xiong Z, Dong F and Yang R. Experimental and numerical studies on laminar premixed flames of ethanol-water-air mixtures. *Energ Fuel* 2014; 28: 4754–4761.
 38. Vancoillie J, Christensen M, Nilsson EJK, Verhelst S and Konnov AA. The effects of dilution with nitrogen and steam on the laminar burning velocity of methanol at room and elevated temperatures. *Fuel* 2013; 105: 732–738.
 39. Lehtiniemi H, Balthasar M, Magnusson I and Mauss F. Modeling diesel spray ignition using detailed chemistry with a progress variable approach. *Combust Sci Technol* 2006; 178: 1977–1997.
 40. Lehtiniemi H, Borg A and Mauss F. Combustion modeling of diesel sprays. SAE technical paper 2016-01-0592, 2016.
 41. Werner A, Netzer C, Lehtiniemi H, Borg A, Matrisciano A, Seidel L, et al. A computational efficient combustion progress variable (CPV) approach for engine applications. In: *Joint meeting of the German and Italian sections of the combustion institute*, Sorrento, 23–26 May 2018. Sorrento, Italy: Combustion Institute.
 42. Kožuch P. *Ein phänomenologisches Modell zur kombinierten Stickoxid- und Russberechnung bei direkt einspritzenden Dieselmotoren*. PhD Thesis, Universität Stuttgart, Stuttgart, 2004.
 43. Hunger M, Böcking T, Walther U, Günther M, Freisinger N and Karl G. Potential of direct water injection to reduce knocking and increase the efficiency of gasoline engines. In: Günther M and Sens M. (eds) *Knocking in gasoline engines*. Cham: Springer, 2018, pp.338–359.
 44. Vaudry A. Thermodynamics of indirect water injection in internal combustion engines: analysis of the fresh mixture cooling effect. *Int J Eng Res* 2018; 20: 527–539.
 45. *Der VDI-Wärmeatlas*. Cham: Springer, 2006.
 46. Bradley D, Morley C, Gu XJ and Emerson DR. Amplified pressure waves during autoignition: relevance to CAI engines. SAE technical paper 2002-01-2868, 2002.
 47. Gu XJ, Emerson DR and Bradley D. Modes of reaction front propagation from hot spots. *Combust Flame* 2013; 133: 63–74.
 48. Netzer C, Seidel L, Pasternak M, Lehtiniemi H, Perlman C, Ravet F, et al. 3D CFD engine knock prediction and evaluation based on detailed chemistry and detonation theory. *Int J Eng Res* 2018; 19(1): 33–44.
 49. Heywood JB. *Internal combustion engine fundamentals*. New York: McGraw-Hill, 1988.
 50. Worm J, Naber J, Duncan J, Barros S and Atkinson W. Water injection as an enabler for increased efficiency at high-load in a direct injected, boosted, SI engine. SAE technical paper 2017-01-0663, 2017.
 51. Teodosio L, De Bellis V and Bozza F. Combined effects of valve strategies, compression ratio, water injection and cooled EGR on the fuel consumption of a small turbocharged VVA spark-ignition engine. SAE technical paper 2018-01-0854, 2018.
 52. Marchitto L, Tornatore C, Costagliola A, Iacobacci A and Valentino G. Effect of water injection on fuel efficiency and gaseous and PN emissions in a downsized turbocharged SI engine. *J Energ Eng* 2018; 144(4): 04018044
 53. Teodosio L, De Bellis V and Bozza F. Water injection: a technology to improve performance and emissions of downsized turbocharged spark ignited engines. SAE technical paper 2017-24-0062, 2017.
 54. Iacobacci A, Marchitto L and Valentino G. Water injection to enhance performance and emissions of a turbocharged gasoline engine under high load condition. SAE technical paper 2017-01-0660, 2017.
 55. Fogla N, Bybee M, Wahiduzzaman S, Millo F and Mirzaeian M. Development of a k-k-e phenomenological model to predict in-cylinder turbulence. SAE technical paper 2017-01-0542, 2017.
 56. Bozza F, De Bellis V, Berni F, D'Adamo A and Maresca L. Refinement of a 0D turbulence model to predict tumble and turbulent intensity in SI engines. Part I: 3D analyses. SAE technical paper 2018-01-0850, 2018.
 57. Bozza F, De Bellis V, Teodosio L, Fontanesi S and Iorio A. Refinement of a 0D turbulence model to predict tumble and turbulent intensity in SI engines. Part II: model concept, validation and discussion. SAE technical paper 2018-01-0852, 2018.